Perirenal White Adipose Tissue Browning and Epithelial-Mesenchymal Transition, Contributes To Tumor Development in Kidney Cancer

Matias Ferrando
Instituto de Medicina y Biología Experimental de Cuyo (IMBECU), Centro Científico y Tecnológico Mendoza, Consejo Nacional de Investigaciones Científicas y Técnicas (CONICET)

Flavia Bruna
Instituto de Medicina y Biología Experimental de Cuyo (IMBECU), Centro Científico y Tecnológico Mendoza, Consejo Nacional de Investigaciones Científicas y Técnicas (CONICET)

Leonardo Romeo
Instituto de Medicina y Biología Experimental de Cuyo (IMBECU), Centro Científico y Tecnológico Mendoza, Consejo Nacional de Investigaciones Científicas y Técnicas (CONICET)

David Contador
Centro de Medicina Regenerativa, Facultad de Medicina, Clínica Alemana, Universidad del Desarrollo, Santiago, Chile

Daiana Moya-Morales
Instituto de Medicina y Biología Experimental de Cuyo (IMBECU), Centro Científico y Tecnológico Mendoza, Consejo Nacional de Investigaciones Científicas y Técnicas (CONICET)

Flavia Santiano
Instituto de Medicina y Biología Experimental de Cuyo (IMBECU), Centro Científico y Tecnológico Mendoza, Consejo Nacional de Investigaciones Científicas y Técnicas (CONICET)

Leila Zyla
Instituto de Medicina y Biología Experimental de Cuyo (IMBECU), Centro Científico y Tecnológico Mendoza, Consejo Nacional de Investigaciones Científicas y Técnicas (CONICET)

Silvina Gomez
Instituto de Medicina y Biología Experimental de Cuyo (IMBECU), Centro Científico y Tecnológico Mendoza, Consejo Nacional de Investigaciones Científicas y Técnicas (CONICET)

Constanza Matilde Lopez-Fontana
Instituto de Medicina y Biología Experimental de Cuyo (IMBECU), Centro Científico y Tecnológico Mendoza, Consejo Nacional de Investigaciones Científicas y Técnicas (CONICET)

Juan Carlos Calvo
Instituto de Biología y Medicina Experimental (IBYME), Consejo Nacional de Investigaciones Científicas y Técnicas (CONICET), Argentina

Rubén Walter Carón
Instituto de Medicina y Biología Experimental de Cuyo (IMBECU), Centro Científico y Tecnológico Mendoza, Consejo Nacional de Investigaciones Científicas y Técnicas (CONICET)

Judith Toneatto
Instituto de Biología y Medicina Experimental (IBYME), Consejo Nacional de Investigaciones Científicas y Técnicas (CONICET), Argentina

Virginia Pistone-Creydt (vpistone@mendoza-conicet.gob.ar)

Instituto de Medicina y Biología Experimental de Cuyo (IMBECU), Centro Científico y Tecnológico Mendoza, Consejo Nacional de Investigaciones Científicas y Técnicas (CONICET)

Research Article

Keywords: human adipose tissue, renal cancer, epithelial-stromal interactions, browning of adipose tissue, epithelial-mesenchymal transition

Posted Date: November 30th, 2021

DOI: https://doi.org/10.21203/rs.3.rs-1021443/v1

Abstract

Tumor cells can interact with neighboring adipose tissue and adipocyte dedifferentiation appears to be an important aspect of tumorigenesis. We evaluated the size of adipocytes in human adipose explants from normal (hRAN) and kidney cancer (hRAT); changes in the expression of WAT and BAT/beige markers in hRAN and hRAT; and changes in the expression of epithelial-mesenchymal transition (EMT) cell markers; in human kidney tumor (786-O, ACHN and Caki-1) and non-tumor (HK-2) epithelial cell lines incubated with the conditioned media (CMs) of hRAN and hRAT. We observed that hRAT adipocytes showed a significantly minor size compared to hRAN adipocytes. Also, we observed that both Prdm16 and Tbx1 mRNA and the expression of UCP1, TBX1, PPARγ, PCG1α, c/EBPα LAP and c/EBPα LIP was significantly higher in hRAT than hRAN. Finally, we found an increase in vimentin and N-cadherin expression in HK-2 cell incubated for 24 h with hRAT-CMs compared to hRAN- and control-CMs. Furthermore, desmin and N-cadherin expression also increased significantly in 786-O when these cells were incubated with hRAT-CMs compared to the value observed with hRAN- and control-CMs. The results obtained, together with the results previously published by our group, allow us to conclude that perirenal white adipose tissue browning and epithelial-mesenchymal transition, contributes to tumor development in kidney cancer.

Introduction

In recent years it has been shown that tumor progression also depends on the bidirectional dialogue between tumor epithelial cells and surrounding stromal cells. Among the different types of cells that share microenvironment with renal epithelial cells, renal adipose tissue is one of the most abundant. Adipose tissue (AT) is mainly responsible for the depository and delivery of energy in response to systemic demands but also is currently recognized as an endocrine and immunomodulating organ that contributes to human physiology, through both systemic and local-specific functions [1]. Cancer cells and cancer associated adipocytes (CAAs) interact with each other, which promotes the formation of a unique microenvironment and stimulates tumor growth and metastasis [2–5]. Therefore, the role of AT on tumor metabolism is becoming increasingly important [6, 7].

Renal cell carcinoma (RCC) is one of the ten most often diagnosed cancers worldwide. Each year over 300000 new RCC cases are diagnosed and nearly 140000 patients die of this disease [8]. RCC is a highly metastatic cancer; nearly 30% of all RCC patients have developed metastasis at the time of diagnosis [9]. Clear cell renal cancer (ccRCC) is the most frequent and aggressive type of RCC, and usually represents 80-85% of all RCC. Furthermore, the incidence of RCC has increased globally by 2–3% per year [10].

Adipocyte dedifferentiation appears to be an important aspect of tumorigenesis [11]. Recent work on breast tissue has shown that the adipocytes that surround tumor epithelial cells undergo a more rapid depletion of their lipid stores than those that are further away from the tumor [12]; and the adipocytes on the invasive front are smaller than those observed at a distance, implying the existence of lipolysis [13;3]. Recently we observed that human perirenal AT fragments from kidney tumor patients (hRAT) expressed significantly higher amounts of the leptin and ObR (leptin receptor) than human perirenal AT fragments from living kidney donors (hRAN) [5]. In addition, leptin can act locally by increasing lipolysis accompanied by a decrease in the size of adipocytes. Therefore, in this work we evaluated the size of adipocytes of hRAN and hRAT.

Two main types of adipose tissue have been described, namely white adipose tissue (WAT) with a classical energy storage function, and brown adipose tissue (BAT) with thermogenic activity [7]. In recent decades, a phenomenon known as ‘browning’ of WAT has been described, which was first reported by Young and colleagues in 1984 [14]. This process is triggered by the increased gene expression levels of different markers involved in the BAT adipogenic differentiation, including PPARG or PGC-1 [15]. The white adipocytes that undergo the browning process are called beige adipocytes. The beige cells of white adipose tissue, as occurs with brown adipocytes, are identified by their multilocular morphology, the

high number of mitochondria, and the expression of a set of genes specific to brown fat such as UCP1, PGC1α, and PRDM16. Although brown and beige cells are morphologically similar and both have the ability to perform thermogenesis, they have different origins and responses to certain stimuli [16]. In recent years, a possible browning process of peritumoral mammary adipose tissue in breast cancer has been postulated. Both due to phenotypic modifications of the peritumoral adipose tissue, and due to changes in the expression of genes involved in the browning process [17-19;7;20]. Gantov *et al.* recently demonstrated that beige adipocytes favor tumor progression of mouse mammary epithelial cell lines, both tumor and non-tumor [20]. Our group recently demonstrated that renal peritumoral AT (hRAT) favors tumor progression through soluble factors that it secretes into the microenvironment, unlike normal renal adipose tissue (hRAN). Thus, hRAT would be able to stimulate a protumorigenic behavior of human renal epithelial cells, both tumor and non-tumor. [5]. Tumor-induced differentiation to beige/brown adipose tissue is an important contribution to the hypermetabolic state of breast cancer [20]. Therefore, we evaluated changes in the expression of WAT and BAT/beige markers in hRAN and hRAT by different methods.

The extracellular matrix (ECM) is a complex structure made up of different proteins, proteoglycans and polysaccharides. Endocrine activity of adipocytes includes several factors implicated in ECM formation and remodeling [21]. We recently observed that conditioned media (MCs) of human adipose explants from kidney cancer (hRAT) increased the metastatic capacity of tumor and non-tumor human renal epithelial cells, unlike hRAN-CMs [5]. The epithelial-mesenchymal transition (EMT) is a characteristic process of epithelial cells when they acquire migratory capacity. Therefore, in this work we decided to evaluate changes in the expression of EMT cell markers characterized by the expression of mesenchymal markers vimentin, desmin and N-cadherin; in human kidney tumor (786-O, ACHN and Caki-1) and non-tumor (HK-2) epithelial cell lines incubated with the CMs of hRAN and hRAT.

Results

The adipocytes that surround the kidney tumor are smaller than the adipocytes that surround a normal kidney.

We evaluate the size of adipocytes from different renal adipose tissues. Specifically, we compared the normal kidney adipose tissue (hRAN) and renal peritumoral adipose tissue (hRAT). We observed significant changes in the size of adipocytes in response to the presence of the tumor. The hRAT adipocytes showed a significantly smaller size compared to the hRAN adipocytes (Fig. 1). This change in adipocyte size, together with the increased expression of leptin and its receptor in hRAT *vs.* hRAN [5], suggest an increase of lipolysis by hRAT adipocytes compared to hRAN adipocytes.

hRAT showed an increase in the gene expression of Prdm16 and TBX1 compared to hRAN.

To evaluate the browning of the perirenal AT, we measured mRNA levels of *Prdm16*, *TBX1*, *Ucp1* and *PGC1 alpha* in AT from normal and tumor kidney. Increased levels of *Prdm16* and *TBX1* mRNA in hRAT compared to hRAN (Fig. 2, $p<0.05$) were found. Although no significant differences were found in *Ucp1* and *PGC1 alpha* mRNA, a tendency to increase was seen in hRAT-CMs (Fig. 2).

UCP1 and PGC1 alpha expression was increased in hRAT adipocytes compared to hRAN.

We performed immunohistochemistry assays on adipose tissue from normal and kidney cancer to measure UCP1, PGC1 alpha and HSP protein levels and localization. UCP1 and PGC1 alpha expression levels increased in hRAT adipocytes compared to hRAN adipocytes (Fig. 3, $p<0.05$).

The expression of UCP1, TBX1, PPARγ, PCG1 alpha, c/EBPα LAP and c/EBPα LIP was significantly higher in hRAT than hRAN.

We evaluated possible changes in the expression of UCP1, TBX1, PPARγ, PCG1α, c/EBPα LAP, c/EBPα LIP, adiponectin and leptin in hRAT and hRAN. We observed an increase in UCP1, TBX1, PPARγ, PCG1α, c/EBPα LAP and c/EBPα LIP and leptin expression in hRAT compared to hRAN ($p<0.05$) (Fig. 4A-F and H). Additionally, we did not observe significant changes in the expression of adiponectin between hRAT and hRAN (Fig. 4G) (Supplementary figure 1).

Soluble factors secreted by hRAT stimulate the expression of EMT cells markers in tumor and non-tumor human kidney cells.

We decided to evaluate changes in the expression of EMT cell markers; in human kidney tumor (786-O, ACHN and Caki-1) and non-tumor (HK-2) epithelial cell lines incubated with the conditioned media (CMs) of human adipose explants from normal (hRAN) and kidney cancer (hRAT) tissue. We found an increase in vimentin and N-cadherin expression in HK-2 cell incubated for 24 h with hRAT-CMs compared to hRAN- and control-CMs ($p<0.05$) (Fig. 5A and I). The same tendency was observed for the expression of desmin, but it was not statistically significant (Fig. 5E). Furthermore, desmin and N-cadherin expression also increased significantly in 786-O when these cells were incubated with hRAT-CMs compared to the value observed with hRAN- and control-CMs (Figure 5F and J, $p<0.05$). However, no significant changes in vimentin expression were observed in 786-0 cells (Fig. 5B). Likewise, we did not find significant changes in the expression of vimentin, desmin or N-cadherin in the two tumor renal epithelial cell lines originating from metastatic sites (ACHN and Caki-1 cells) (Fig. 5C-D, G-H and K-L) (Supplementary figure 2).

Discussion

Renal cancer (RCa) is considered to be the fifth most common type of cancer worldwide, having a high mortality rate in both men and women. In Argentina, 4100 new cases are diagnosed each year in both sexes, being more frequent in men. Tumor development and maintenance of a cancerous phenotype, requires a bidirectional communication between epithelial cells and the stromal environment. Renal adipose tissue is one of the most abundant cell types surrounding renal epithelial cells. This tissue is a bioactive endocrine organ that secretes soluble factors and contributes significantly to the composition of the extracellular matrix. Our group has shown that the periprostatic adipose tissue of patients with prostate cancer can regulate the behavior of the tumor, both in the early and late stages of the disease [23]. Furthermore, we have worked with adipose tissue fragments from human breast tumors (hATT) and normal breast glands (hATN), from which we obtained the corresponding conditioned media (hATT-CMs and hATN-CMs). We show that hATT is capable of stimulating the growth and metastatic capacity of mammary tumors by different mechanisms, unlike hATN [24;3;25]. Recently, we demonstrated that renal peritumoral adipose tissue undergoes a process of adaptation to changes locally generated by the tumor [5]. Also, we show that this hRAT is capable of stimulating a protumorigenic behavior of renal epithelial cells. We observed that hRAT expresses significantly higher amounts of leptin and ObR, relative to hRAN. It has been shown that leptin has a pro-tumorigenic function and act locally by increasing lipolysis. This increase in lipolysis is accompanied by a decrease in the size of adipocytes. Along these lines, our results show a significant decrease in the mean size of hRAT adipocytes with respect to the size of hRAN adipocytes (Fig. 1). The increased expression of both leptin and its receptor, together with the decrease in the size of hRAT adipocytes, allow us to suggest an increase in lipolysis in hRAT adipocytes. The increase in lipolysis would allow a greater availability of energy to the tumor, favoring its development.

Adipocytes are the main stromal cells in the mammary microenvironment, and crosstalk between adipocytes and cancer cells may play a critical and important role in cancer maintenance and progression. Tumor induced differentiation to beige/brown adipose tissue is an important contribution to the hypermetabolic state of breast [20] and prostate [7] cancer, but still the bibliography says nothing about browning and kidney cancer. And, the effect of epithelial cell-beige adipocyte communication on tumor progression remains unclear. To begin to elucidate this, we evaluated the expression of different markers WAT and BAT / beige adipocytes in hRAT and hRAN. The browning of WAT is triggered by the increased gene

expression levels of different markers involved in the BAT adipogenic differentiation, including PPAR gamma or PGC-1 alpha [26]. Also, PPAR gamma induces the expression of C/EBP, which makes this gene a key regulator of WAT differentiation [27]. PPAR gamma also induces the expression and production of UCP-1 in these beige adipocytes [28]. UCP1 this transmembrane protein uncouples the electron transport chain (ETC) by pumping protons from the intermembrane space back into the mitochondrial matrix, thereby generating heat rather than ATP [29]. As well, PRDM16 is a master regulator gene of brown adipocyte differentiation and TBX1 beige adipocyte marker [18]. We observed that both Prdm16 and Tbx1 genes and the protein expression of UCP1, TBX1, PPARγ, PCG1α, c/EBPα LAP and c/EBPα LIP was significantly higher in hRAT than hRAN (Fig. 2-4). This is the first work that demonstrates a transdifferentiation of WAT adipocytes in the human perirenal AT that surrounds a renal tumor, since we observed an increase in the amount of beige adipose tissue in hRAT, as opposed to the hRAN. In light of these results, together with those previously described [5], we postulate that the renal tumor would be regulating the differentiation of the surrounding WAT and its browning. The browning process might have a role in the development of kidney tumors. Nowadays, and to deepen this possible regulation, we set out to study changes in WAT and BAT/beige adipocytes markers in hRAN fragments incubated with MCs from tumor kidney cell lines. Preliminary results allow us to observe an increase in the expression of BAT/beige adipocyte markers in hRAN, which would support the hypothesis that the renal tumor would be stimulating the browning of the surrounding TA.

Finally, we evaluate the ability of hRAT- and hRAN-CMs to produce changes in the expression of EMT cell markers; in human kidney tumor and non-tumor epithelial cell lines incubated with the MCs of hRAN and hRAT. Previosuly we showed that hRAT expresses significantly higher amounts of leptin and ObR, relative to hRAN [5]. It has been described that leptin induces a fibroblastoid morphology evidenced by the decrease in the expression of epithelial markers (occludin, E-cadherin) and an increase in mesenchymal markers (fibronectin, N-cadherin, and vimentin) in breast cancer [30]. In accordance with our previous results, where we observe that hRAT-CMs increased the metastatic capacity of tumor and non-tumor human renal epithelial cells, we found an increase in vimentin and N-cadherin expression in HK-2 cell, desmin and N-cadherin expression in 786-O cells incubated with hRAT-CMs compared to hRAN- and control-CMs. Likewise, it has been described that leptin is capable of stimulating EMT. And we previously demonstrated that hRAT expresses higher amounts of leptin than hRAN. ECM remodeling in pathological processes included obesity and tumor progression, since it needs to undergo a reorganization to allow accommodation of the hypertrophic adipocytes allowing access to the lipid content of adipocytes [31]. During the tumor progression, ECM remodeling is a key factor involved that allow invasion and cell migration [32]. Endocrine activity of adipocytes includes several factors implicated in ECM formation and remodeling through switch on the synthesis and release of molecules such as collagenases and/or metalloproteinases, favoring a better environment for cell migration out of the primary tumor [7]. Therefore, we postulate that this adipokine could be involved in increasing the expression of EMT markers. It is striking to see this increase in the non-tumor cell line.

This is the first report demonstrating that human adipose tissue from renal tumor (hRAT) presents beige/brown adipocyte characteristics, unlike human adipose tissue from normal renal (hRAN). This browning process could be stimulated by the kidney tumor itself, and play an important role in renal tumor development. Furthermore, we demonstrate that hRAT produces soluble factors that stimulate the metastatic capacity of both tumor and non-tumor human kidney cells.

Methods

Reagents

Reagents were from Sigma Chemical Co (St. Louis, MO, USA), tissue culture flasks, dishes, and multi-well plates were from Falcon Orange Scientific (Graignette Business Park, Belgium), and culture media from both tissue and cell lines and supplements were from Gibco BRL (Carlsbad, CA, USA) [3-5].

Sample collection and handling

Human adipose tissue explants from cancerous (hRAT; n=23) kidneys were obtained from patients to whom a partial or total (tumor) nephrectomy was performed. Human adipose tissue explants from normal kidneys (hRAN; n=19), were obtained from live kidney donors who had not received previous chemotherapy or radiotherapy treatment. The median of body mass index (BMI) of patients was: 26.8 kg/m^2 for patients with renal tumor (hRAT), and 24.9 kg/m^2 for living kidney donors (hRAN). (BMI) (kg/m2) was calculated as weight (kg) divided by height (m) squared.

Samples were transported in PBS and processed immediately. On average, 2 h elapsed from the acquisition of the surgical sample until it was processed under a sterile laminar flow hood. The project was approved by the Medical School's ethics committee (Universidad Nacional de Cuyo, Argentina) according to Declaration of Helsinki to experimentation with human subjects. All patients gave their informed consent to undergo tissue harvesting for this research [5].

Gene expression by RT-qPCR analysis

Total RNA was extracted from 100mg of tissue using Trizol reagent (Invitrogen, Carlsbad, CA, USA) and quantified according to its absorbance at 260nm (NanoDrop 2000, Thermo Scientific, Wilmington, USA). Contaminating genomic DNA was degraded with DNAse RQ1 (Promega, Madison, USA), cDNA was synthesized from one microgram of total RNA using 300pmol oligo-dT primers, 10mM dNTP (Thermo Scientific, Wilmington, USA) and 200U M-MLV reverse transcriptase (Promega, Madison, USA). Real-time PCR was performed in a final volume of 20 uL containing 50 ng cDNA, 3mM MgCl2, PCR LightCycler-DNA Master SYBRGreen reaction mix (Roche, Indianapolis, USA) and 0.5 mM of each specific primers (Table 1). Amplification was performed in a using LightCycler thermocycler (Roche, Indianapolis, USA). Controls without reverse transcription were included to ensure that amplifications were from mRNA and not from genomic DNA. Amplicons were characterized according to their melting temperature and size. The mRNA level of each target gene was calculated using the 2ΔΔCt method and normalized against the mRNA of β-actin [4-5].

Table 1: primer pair sequence are shown for the Forward (F) and Reverse (R) primers used to measure mRNA abundance by RT-qPCR

Gen	Forward (5´-3´)	Reverse (5´-3´)	Ct	Size (pb)	TM (°C)	Gene bank
Prdm16	GGCAAACGCTTCGAATGTGA	ACCGTGCTGTGGATATGCTT	35	173	94	NM_199454.2
Tbx1	ACGACAACGGCCACATTATTC	CCTCGGCATATTTTCTCTATCT	35	102	85	AF012131.1
Ucp1	GCAGGGAAAGAAACAGCACCTA	TCCCTTTCCAAAGACCCGTCAA	35	217	86	NM_021833.4
Pgc1 alpha	ACCAGCCAACACTCAGCTAA	AGGGACGTCTTTGTGGCTTT	35	170	83	NM_013261.3
GAPDH	GGAGCGAGATCCCTCCAAAAT	GGCTGTTGTCATACTTCTCATGG	40	197	89	NM_002046.3

H&E staining

Tissues (hRAT and hRAN) were fixed in 4% formaldehyde and embedded in paraffin. They were afterwards cut into sections of 3 μm thickness with a microtome, deparaffinized and stained with hematoxylin-eosin (H&E). Images were taken with a Nikon Eclipse E200 Microscope fitted with a digital still camera Micrometric SE Premium (Nikon Corp.,

Japan) at 100x magnification. Adipocyte area quantification (measuring adipocyte perimeter) in the three tissue types was performed in 8–10 fields of each preparation as mentioned above [5].

Immunohistochemistry

10 µm serial cuts were performed on the same tissue samples embedded in paraffin used for H&E staining. UCP1, PGC1 alpha and HSP expression were studied by means of immunohistochemistry. Briefly, hRAN and hRAT microtome slides were first deparaffinized, and then a heat-mediated antigen retrieval, endogenous peroxidase blocking and nonspecific tissue blocking were performed. Slides were then incubated with the different primary antibodies at 4 °C, and after that with an anti-rabbit biotinylated secondary IgG antibody. Finally, slides were incubated with peroxidase-conjugated streptavidin. Peroxidase reaction was performed with chromogen 3,3'-diaminobenzidine (DAB) (DAKO LSAB + Kit, HRP). Hematoxylin counter stain was performed. Serial cuts incubated in the absence of primary antibody were used as negative controls. Images were taken with a Nikon Eclipse E200 Microscope fitted with a Micrometric SE Premium (Nikon Corp., Japan) digital still camera at 100x and 400x magnification. DAB staining quantification in the three tissue types was performed in 5 fields of each preparation as mentioned above [3-5].

Preparation of conditioned media (CMs) from hRAN and hRAT

Adipose tissues were washed with cold PBS and weighed. hRAN or hRAT were plated in culture flask with M199 culture medium (Invitrogen™; 1 g tissue/10 ml M199), supplemented with gentamicin (50 µg/ml) and incubated for 1 h at 37 ºC in 5 % CO_2. After that, the medium was removed and replaced with fresh medium and the tissues were incubated for 24 h. Subsequently, the supernatant was collected and filtered using filters with 0.22 µm membranes. Then, supernatants were aliquoted into 1-ml fractions and immediately stored at -80 ºC. The control-CMs were obtained from the collection of serum-free M199 medium after 24 h of incubation in a culture flask at 37 ºC in 5 % CO_2 [5].

Treatment with hRAN- and hRAT-CMs

In order to study the EMT proteins expression of tumor (786-O, ACHN and Caki-1) and non-tumor (HK-2) human renal epithelial cell lines, MCs collected were diluted 1:1 in DMEM-F12 (Invitrogen, UK) 2 % fetal bovine serum (FBS; 1 % FBS final concentration) and the cells were incubated for 24 h with the diluted CMs. The experiments were performed with equal volumes of hRAN- and hRAT-CMs. The concentration of total protein in those volumes was quantified using Bradford reagent [4-5].

Culture of tumor and non-tumor renal epithelial cell lines

Tumor (786-O, ACHN and Caki-1) and non-tumor (HK-2) human renal epithelial immortalized cell lines were used. 786-O (ATCC® CRL1932™), ACHN (ATCC® CRL1611™), Caki-1 (ATCC® HTB46™) and HK-2 (ATCC® CRL2190™) were obtained from the American Type Culture Collection (ATCC, Rockville, MD). 786-O is a line derived from a primary clear cell adenocarcinoma (primary tumor); and both ACHN and Caki-1 are lines derived from metastatic sites (pleural effusion and skin respectively). The four cell lines were cultured in DMEM-F12 medium with 10 % FBS and 2 µg/ml insulin; and were maintained at 37 ºC in 5 % CO_2 [5].

Preparation of cell lysates from renal epithelial cells after incubation with hRAN-, hRAT- or control-CMs

786-O, ACHN, Caki-1 and HK-2 cells were seeded in six-well plates in DMEM-F12 complete medium. When cells reached 75-80 % confluence, the medium was aspirated and cells were washed twice with PBS. Then, cells were incubated at 37 ºC for 24 h either with hRAN-, hRAT- or control-CMs (50% CM, 50% DMEM-F12 2% FSB). Cells were lysed with Ripa buffer (Tris 10mM pH 7,5; NaCl 150mM; sodium vanadate 2mM; sodium deoxycholate; SDS 0,1%; igepal 1%; protease inhibitors), pelleted by centrifugation at 4 ºC and stored at -80 ºC [4-5].

Western Blot analysis

In order to evaluate protein expression levels, Western blots were performed. UCP1, TBX1, PPARγ, PCG1α, c/EBPα LAP, c/EBPα LIP, adiponectin, leptin, vimentin, desmin and N-cadherin were measured after incubation of the epithelial cell lines with the different CMs obtained. In order to lyse cells, Ripa buffer was used. Total protein in samples was quantified by Bradford method. Proteins were separated in a SDS-PAGE 12 gel, and electrotransferred to a nitrocellulose membrane (Amersham). The membrane was later blocked with bovine serum albumin (Sigma-Aldrich, 0055K) and then incubated with the different antibodies ON at 4ºC. The membranes were later washed, and incubated with proper secondary antibodies conjugated with biotione, and subsequently the signal was amplified with streptovidin. Antibody complexes were visualized by means of chemiluminescence (ECL; GE Helathcare). Bands were quantified by densitometry using FIJI Image processing package [22]. In the cell extracts, β-actin level in samples was used to determine that equal quantities of proteins were loaded in the gel [3-5].

Statistical methods

The statistical significance between different experimental conditions was evaluated by *t*-test or one-way ANOVA. Tukey´s post-hoc tests were performed within each individual treatment. The results are presented as mean ± SEM. Results were considered significant at $p < 0.05$.

Declarations

Acknowledgements

This study was partially supported by grants to Dr. Virginia Pistone Creydt: Subsidio para Investigación Médica 2017-2019 from Fundación Roemmers; Subsidio para promoción de la Investigación, SIIP 2019-2020, Universidad Nacional de Cuyo; Subsidio Proyectos de Investigación Científica y Tecnológica (PICT), Agencia Nacional de Promoción de la Investigación, el Desarrollo Tecnológico y la Innovación, 2021-2023.

The authors declare that they have no conflict of interest.

Author contributions

MF performed research, analyzed data and contributed with the manuscript draft. FAB performed research, analyzed data and contributed with the manuscript draft. LRR contributed with part of the biological samples used and the manuscript draft. DC, DLMM, FES, LEZ, SG and CMLF performed research and contributed to the discussion of the results. JCC participated in coordinating and drafting the manuscript. RWC designed research and helped draft the manuscript. JT designed research and helped draft the manuscript. VPC designed research, performed research, analyzed data and wrote the paper. All authors read and approved the final manuscript.

Competing interests

The authors declare that they have no competing interests.

References

1. Hassan, M. & Magdi Yacoub, N. L. Adipose tissue: friend or foe? *Nat Rev Cardiol*, **9**, 689–702 (2012).
2. Duong, M. N. *et al.* The fat and the bad: Mature adipocytes, key actors in tumor progression and resistance. *Oncotarget*, **8**, 57622–41 (2017).

3. Fletcher, S. J. *et al.* Human breast adipose tissue: characterization of factors that change during tumor progression in human breast cancer. *J Exp Clin Cancer Res*, **36**, 26 https://doi.org/doi: 10.1186/s13046-017-0494-4 (2017).
4. Campo-Verde-Arbocco, F. *et al.* Human renal adipose tissue induces the invasion and progression of renal cell carcinoma. *Oncotarget*, **8**, 94223–34 https://doi.org/doi: 10.18632/oncotarget.21666 (2017).
5. Bruna, F. A. *et al.* Human renal adipose tissue from normal and tumor kidney: its influence on renal cell carcinoma. *Oncotarget*, **10**, 10:5454–67 https://doi.org/doi: 10.18632/oncotarget.27157 (2019).
6. Diedrich, J., Gusky, H. C. & Podgorski, I. Adipose tissue dysfunction and its effects on tumor metabolism. *Horm Mol Biol Clin Investig*, **21**, 17–41 https://doi.org/doi: 10.1515/hmbci-2014-0045 (2015).
7. Álvarez-Artime, A., García-Soler, B., Sainz, R. M. & Mayo, J. C. Emerging Roles for Browning of White Adipose Tissue in Prostate Cancer Malignant Behaviour. *Int J Mol Sci*, **22**, 5560 https://doi.org/doi: 10.3390/ijms22115560 (2021).
8. Capitanio, U. *et al.* Epidemiology of Renal Cell Carcinoma. *Eur Urol*, **75**, 74–84 (2019).
9. Bhatt, J. R. & Finelli, A. Landmarks in the diagnosis and treatment of renal cell carcinoma. *Nat Rev Urol*, **11**, 517–525 (2014).
10. Padala, S. A. *et al.* Epidemiology of Renal Cell Carcinoma. *World J Oncol*, **11**, 79–87 https://doi.org/doi: 10.14740/wjon1279 (2020).
11. Martinez, J. & Cifuentes, M. Adipose tissue and desmoplastic response in breast cancer. Breast cancer, carcinogenesis, cell growth and signalling pathways (ed. Mehmet G) 447–56 (Washington: National Academies Press, 2011)
12. Hovey, R. C. & Aimo, L. Diverse and active roles for adipocytes during mammary gland growth and function. *J Mammary Gland Biol Neoplasia*, **15**, 279–290 (2010).
13. Brasaemle, D. L., Dolios, G., Shapiro, L. & Wang, R. Proteomic analysis of proteins associated with lipid droplets of basal and lipolytically stimulated 3T3-L1 adipocytes. *J Biol Chem*, **279**, 46835–42 https://doi.org/doi: 10.1074/jbc.M409340200 (2004).
14. Young, P., Arch, J. R. S. & Ashwell, M. Brown Adipose Tissue in the Parametrial Fat Pad of the Mouse. *FEBS Lett*, **167**, 10–14 (1984).
15. Puigserver, P. *et al.* A. Cold-Inducible Coactivator of Nuclear Receptors Linked to Adaptive Thermogenesis., **92**, 829–839 (1998).
16. Chu, D. T. & Gawronsha-Kozak, B. Brown and brite adipocytes: same function, but different origin and response., **138**, 102–105 (2017).
17. Wang, F. *et al.* Mammary Fat of Breast Cancer: Gene expression Profiling and Functional Characterization. *PLoS ONE*, **9**, e109742 (2014).
18. Singh, R. *et al.* Increased expression of Beige/Brown adipose markers from host and breast cancer cells influence xenograft formation in mice. *Mol Cancer Res*, **14**, 78–92 (2016).
19. Elsen, M. *et al.* BMP4 and BMP7 induce the white-to-brown transition of primary human adipose stem cells. *Am J Physiol Cell Physiol*, **306**, C431–C440 (2015).
20. Gantov, M. *et al.* Beige adipocytes contribute to breast cancer progression. *Oncol Rep*, **45**, 317–328 https://doi.org/doi: 10.3892/or.2020.7826 (2021).
21. Occhino, F. & Stehulak, T. Behind the Slow Pace of Wage Growth. *Economic Trends*, **115**, 8–10 (2015).
22. Gati, A. *et al.* Obesity and renal cancer: Role of adipokines in the tumor-immune system conflict. *Oncoimmunology*, **1;3**, e27810 (2014).
23. Sacca, P. A. *et al.* Human periprostatic adipose tissue: its influence on prostate cancer cells. *Cellular Physiology and Biochemistry*, **30**, 113–122 (2012).

24. Pistone Creydt, V. *et al.* Human adipose tissue from normal and tumoral breast regulates the behavior of mammary epithelial cells. *Clin Transl Oncol*, **15**, 124–131 (2013).
25. Fletcher, S. J. *et al.* Comparative proteomics of soluble factors secreted by human breast adipose tissue from tumor and normal breast. *Oncotarget*, **24;9**, 31007–17 https://doi.org/doi:10.18632/oncotarget.25749 (2018).
26. Nedergaard, J. & Cannon, B. The browning of white adipose tissue: some burning issues. *Cell Metab*, **20**, 396–407 https://doi.org/doi: 10.1016/j.cmet.2014.07.005 (2014).
27. Tanaka, T., Yoshida, N., Kishimoto, T. & Akira, S. Defective Adipocyte Differentiation in Mice Lacking the C/EBPβ and/or C/EBP. Gene. *EMBO J*, **16**, 7432–43 (1997).
28. Chawta, A., Repa, J. J., Evans, R. M. & Mangelsdorf, D. J. Nuclear Receptors and Lipid Physiology: Opening the x-Files., **294**, 1866–70 (2001).
29. Fedorenko, A., Lishko, P. V. & Kirichok, Y. Mechanism of Fatty-Acid-Dependent UCP1 Uncoupling in Brown Fat Mitochondria., **151**, 400–413 (2012).
30. Olea-Flores, M., Juárez-Cruz, J. C., Mendoza-Catalán, M. A. & Padilla-Benavides, T. Navarro-Tito, N. Signaling Pathways Induced by Leptin during Epithelial–Mesenchymal Transition in Breast Cancer. *Int J Mol Sci*, **19**, 3493 https://doi.org/doi: 10.3390/ijms19113493 (2018).
31. Schoettl, T., Fischer, I. P. & Ussar, S. Heterogeneity of Adipose Tissue in Development and Metabolic Function. *J. Exp. Biol.* **7**:221(Pt Suppl 1):jeb162958. doi: 10.1242/jeb.162958 (2018)
32. Walker, C. & Mojares, E. Del Río Hernández, A. Role of Extracellular Matrix in Development and Cancer Progression. *Int. J. Mol. Sci*, **19**, 3028 https://doi.org/doi: 10.3390/ijms19103028 (2018).

Figures

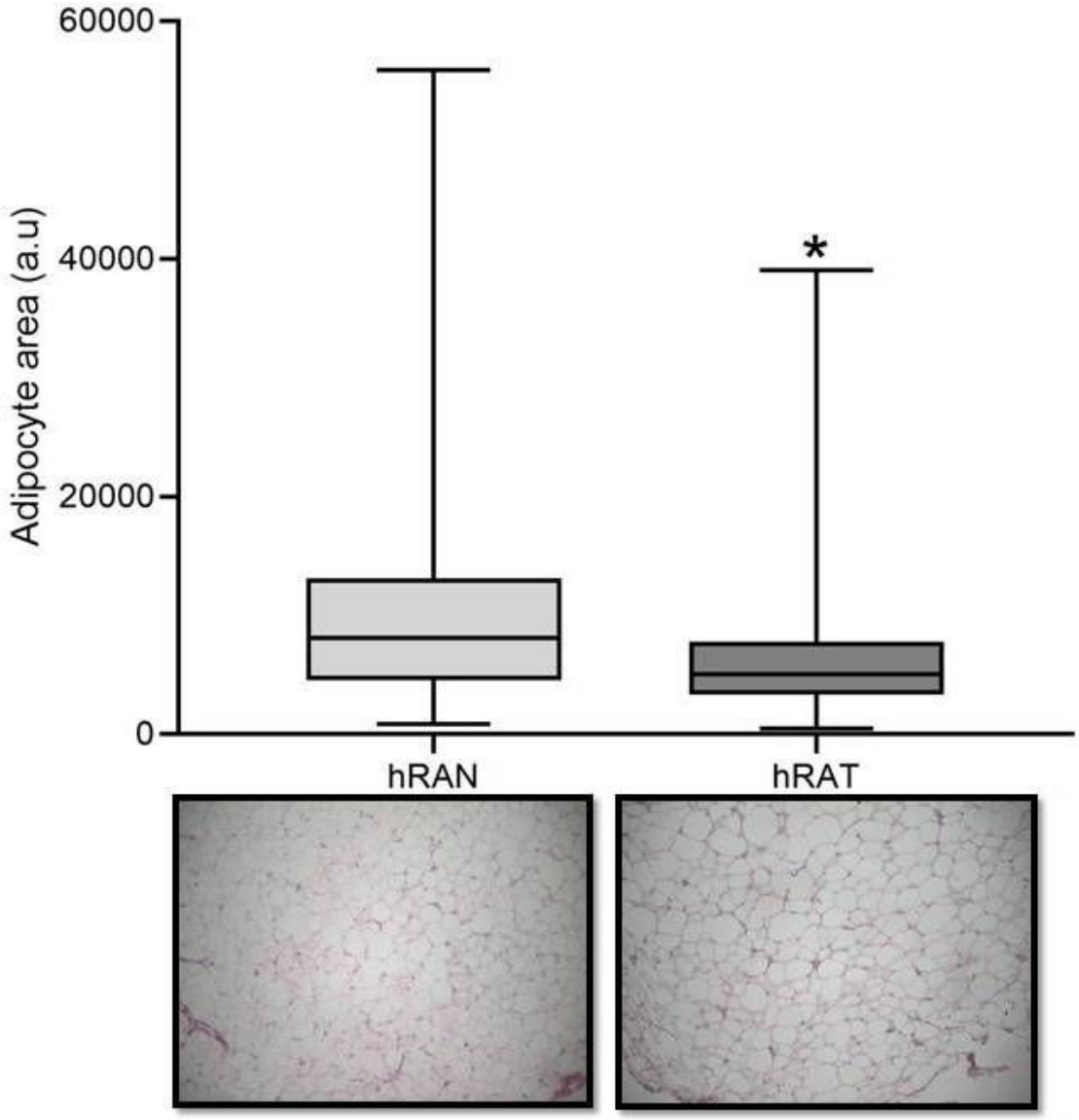

Figure 1

Microscopic evaluation of different renal adipose tissues. Slides from adipose tissue samples from normal kidney of hRAN; and tissue samples of tumor kidney attached to the tumor of hRAT. Adipose tissue fragments were cut in paraffin, stained with H&E, and observed under light microscope. Adipocyte size was quantified with Image J software (NIH). The graphic show median ± SEM of two independent experiments. *p < 0.05 hRAT attached to the tumor vs. hRAN. Magnification: 100X.

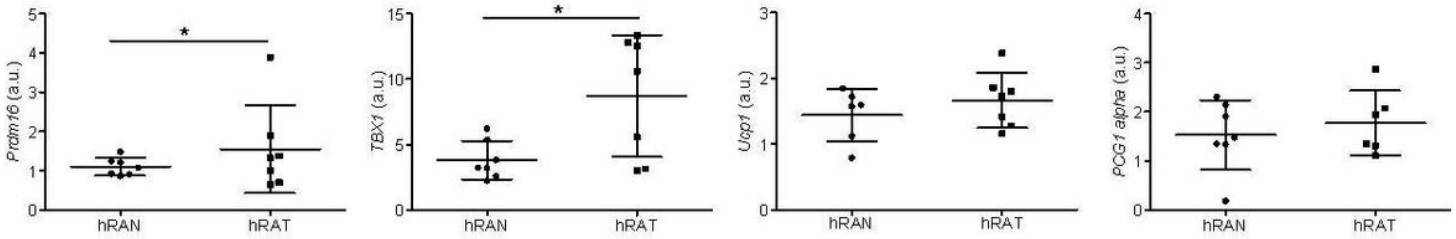

Figure 2

Relative fold expression of Prdm16, TBX1, Ucp1 and PGC1 alpha gene expression from hRAN and hRAT. The mRNA profiles of Prdm16, TBX1, Ucp1 and PGC1 alpha from different adipose tissue were analyzed by qRT-PCR and normalized by their relative ratio to GAPDH. Data are mean ± SEM. GAPDH, glyceraldehyde-3-phosphate dehydrogenase. *p<0.05.

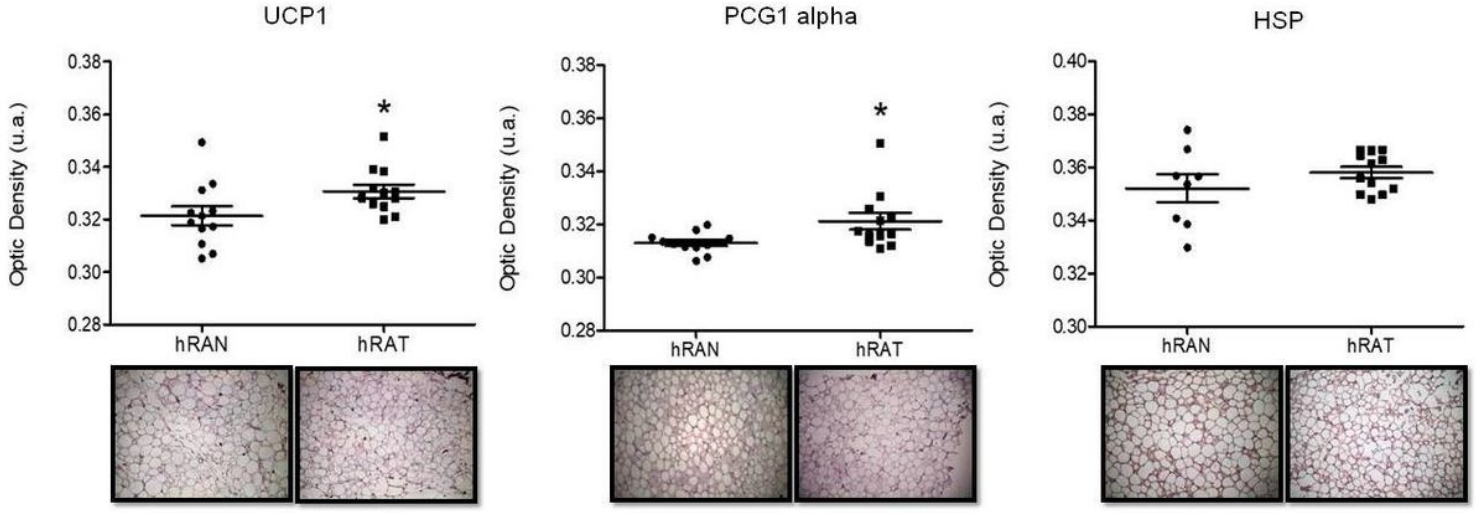

Figure 3

UCP1, PGC1 alpha and HSP expression in in histological sections of hRAN and hRAT. UCP1, PGC1 alpha and HSP expression was evaluated by immunohistochemistry in serial cuts of hRAN and hRAT. DAB staining quantification in the three tissue types was performed with Image J software (NIH). Histograms show mean ± SEM of five independent experiments. (a.u.: arbitrary units). *p < 0.01 hRAN vs. hRAT. Representative photographs of hRAN- and hRAT-staining. Magnification: ×100.

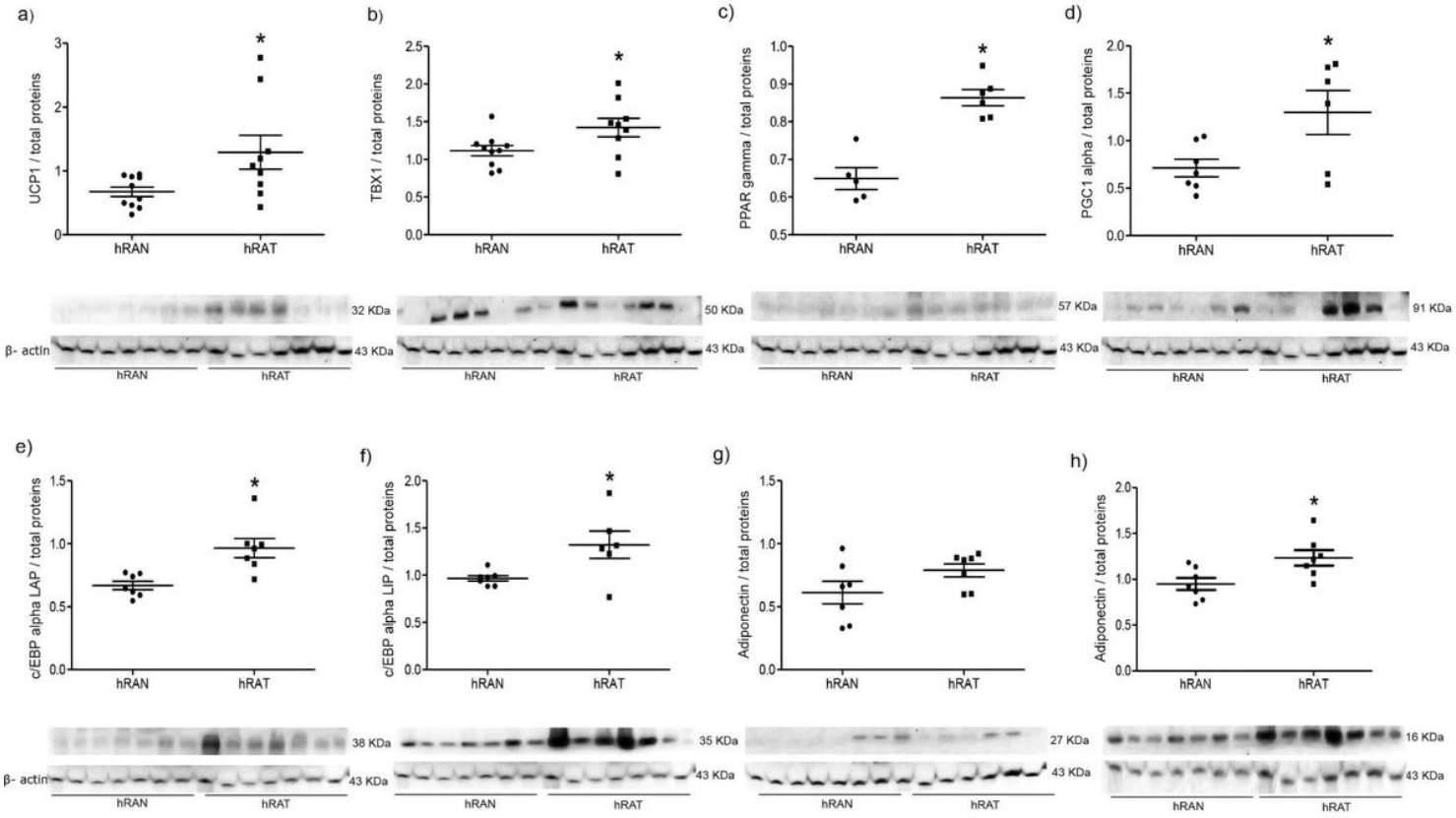

Figure 4

UCP1, TBX1, PPARγ, PCG1 alpha, c/EBPα LAP, c/EBPα LIP, adiponectin and leptin in tissue lysate of hRAN and hRAT. UCP1, TBX1, PPARγ, PCG1 alpha, c/EBPα LAP, c/EBPα LIP, adiponectin and leptin expression was evaluated by Western blot. Images were analyzed by densitometry. Horizontal bars represent the geometric mean of each data set. Vertical bars indicate SEM. *$p < 0.05$ hRAN vs. hRAT.

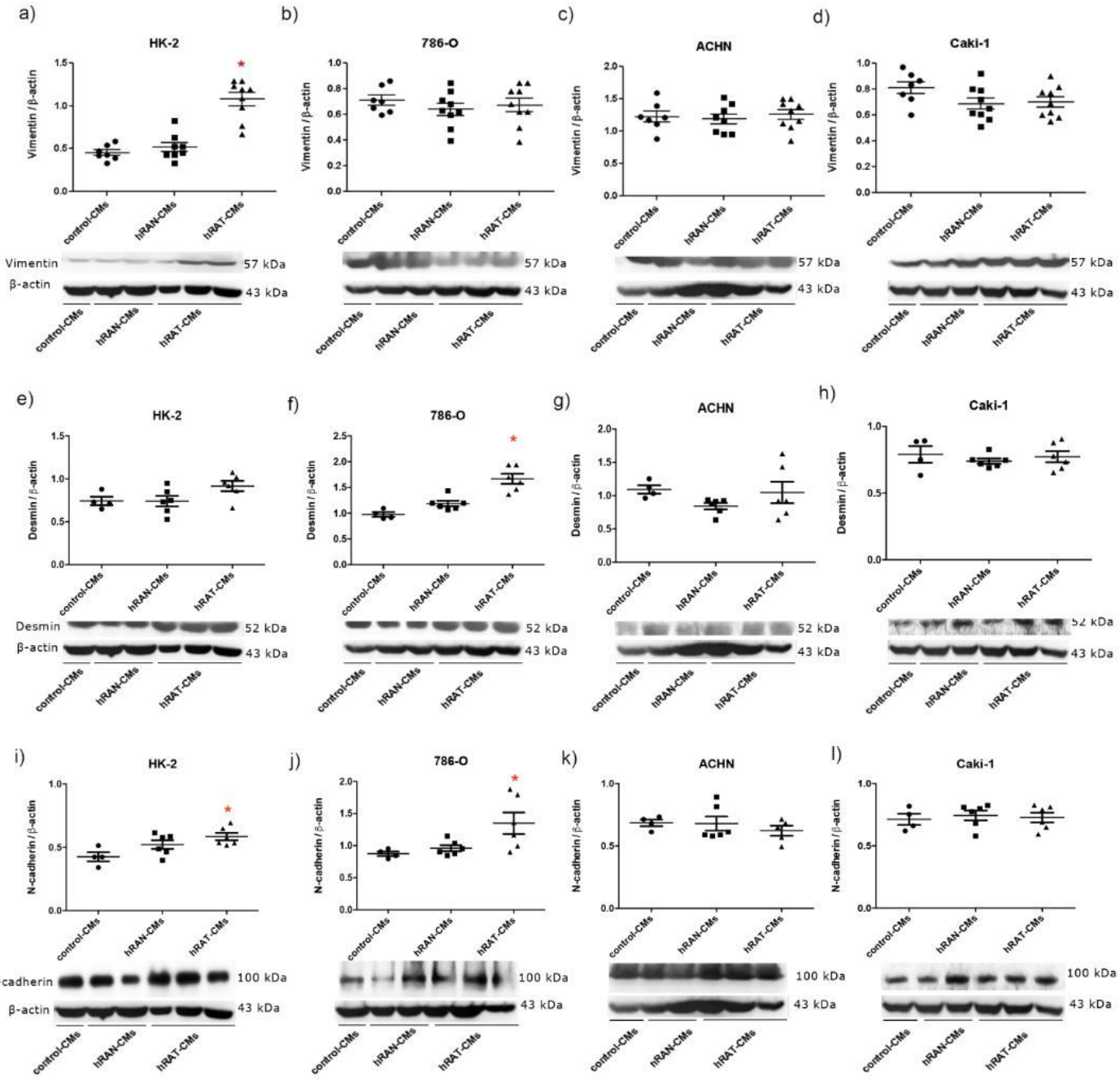

Figure 5

Effect of CMs from hRAN and hRAT on: vimentin (a-d); desmin (e-h), and N-cadherin (i-l) expression was evaluated in HK-2, 786-O, ACHN and Caki-1 cell lines. HK-2, 786-O, ACHN and Caki-1 cells were grown on 6 well plates, incubated for 24 hs with the different CMs and then lysed. Expression of the different proteins was measured by Western blot. β-actin was used as internal control. Images were analyzed by densitometry. Horizontal bars represent the geometric mean of each data set. Vertical bars indicate SEM. *p < 0.05 cells incubated with hRAT-CMs vs. hRAN-CMs and control-CMs.

Supplementary Files

This is a list of supplementary files associated with this preprint. Click to download.

- Supplementaryfigure1withlegend.png

- Supplementaryfigure2withlegend.png